Method of Statistical Analysis of Enroute Airspace Pairwise Flight Performance

Ashim Kumar Thapa*
Center for Air Transportation Systems Research
George Mason University, Fairfax, Virginia, 22030
ORCID: https://orcid.org/0009-0003-7939-4152
Email: athapa26@gmu.edu

Lance Sherry
Director, Center for Air Transportation Systems Research
Professor, Systems Engineering and Operations Research Department
George Mason University, Fairfax, Virginia, 22030
Email: lsherry@gmu.edu

Total Number of Pages: 20

Submitted [8/1/2026]
*Corresponding Author

ABSTRACT

Objectives: Accurately monitoring aircraft-to-aircraft proximity in enroute airspace is essential for verifying that separation standards are maintained as traffic volume grows. The objective of this research is to develop and apply a systematic, statistical proximity ("breach") event analysis method using open-source surveillance data. The method includes a statistical approach to detecting, classifying, and characterizing pairwise aircraft proximity events in enroute airspace, and to quantify how breach frequency and severity vary over time and region.

Methods: ADS-B data for the bounded Washington, D.C. enroute airspace were processed using a 22-step methodology for the year 2025. Detected breaches were classified by severity (<3 NM, <5 NM, <10 NM), flight direction, lateral state, and vertical state. Outputs include separation histograms, severity bar charts, hotspot heatmaps, and seasonal/monthly boxplots. Kruskal-Wallis and post-hoc Dunn's tests were used to assess seasonal and monthly variation in daily breach counts.

Findings: To demonstrate the method, the traffic in the Washington DC airspace was analyzed for one day (January 1, 2025) and for a sequence of 304 days in 2025.The <3 NM threshold occurred on 9 days (mean 3 breaches/day, maximum 8); the <5 NM threshold on 36 days (mean 4, maximum 41); and the <10 NM threshold on all days of the 2025 year (mean 874, maximum 1,892). Daily breach counts varied significantly by season and month, with Summer showing the lowest median, minimum, and maximum counts among seasons, and September the lowest median among months.

Novelty: This paper presents an end-to-end, open-source data pipeline for analysis of pairwise flight performance, combining staged proximity pre-filtering, geographic hotspot mapping, and nonparametric statistical testing for enroute airspace.

Practical Applications: The method gives regulators and air navigation service providers a replicable tool for continuous separation-risk monitoring and for targeting geographic and seasonal differences warranting alternate safety review for en-route operations.

1. INTRODUCTION

Enroute airspace operations constitute the backbone of the global air transportation network, managing the safe and efficient transit of aircraft cruising between Terminal Areas.

Within this domain, Air Traffic Management (ATM) frameworks rely heavily on strict geometric and procedural thresholds to maintain safe buffers between aircraft. The required minimum separation distance between aircraft is considered a critical limiting factor on overall airspace capacity (Pérez Maroto et al. 2022). As air traffic volume continues to scale, understanding how these separation standards are calculated, monitored, and structurally adjusted becomes paramount to optimizing throughput without compromising the structural safety of the National Airspace System (NAS).

To systematically mitigate the risk of midair collisions, the Federal Aviation Administration (FAA) and the International Civil Aviation Organization (ICAO) mandate specific lateral, longitudinal, and vertical separation criteria. Historically, standard enroute separation within domestic radar-controlled airspace required a minimum horizontal buffer of 5 nautical miles (NM) and a vertical interval of 2,000 feet Required Vertical Separation Minima (RVSM) (Federal Aviation Administration 2022). This baseline structure guarantees that localized positioning errors, sensor lag, or sudden environmental perturbations do not result in catastrophic close encounters or operational errors.

Advancements in surveillance technologies and digital avionics have prompted regulatory updates that allow for a controlled reduction of these separation margins. A notable example is the implementation of Reduced Vertical Separation Minimum (RVSM), which halved the required vertical separation to 1,000 feet between flight level (FL) 290 and FL 410 inclusive for qualified aircraft (Federal Aviation Administration 2022).

Modern frameworks increasingly exploit advanced capabilities like Automatic Dependent Surveillance-Broadcast (ADS-B) to transition from static, conservative boundaries to highly dynamic trajectory management models (Pérez Maroto et al. 2022). These data-driven innovations significantly diminish structural delays, reduce fuel burn, and safely expand the operational capacity of contemporary high-altitude airspace.

Accurately tracking aircraft separation within specified enroute airspace is vital to maintaining operational safety, preventing midair collisions, and optimizing airspace capacity as traffic density increases (Pérez Maroto et al. 2022). Traditional air traffic management has historically relied on localized radar infrastructure to enforce conservative minimum separation margins. However, the global proliferation of Automatic Dependent Surveillance-Broadcast (ADS-B) technology provides a highly precise, state-vector alternative that broadcasts real-time positioning information once per second (Federal Aviation Administration 2022). This technological paradigm shift creates an unprecedented opportunity for researchers to utilize massive, open-source flight-tracking datasets—such as those compiled via grassroots receiver networks—to independently analyze pairwise aircraft proximity and identify potential localized bottlenecks or systemic standard violations (Jansen 2020). By leveraging these open-source resources, modern data-driven methodologies can model complex high-altitude trajectory patterns, validate the efficacy of existing separation standards, and safely pave the way for dynamic, capacity-expanding airspace management frameworks.

This paper describes the metrics and methods for statistically calculating separation distance breaches in enroute airspace (Section 3). A case study is provided for the Washington DC airspace in Section 4. The implications of the method, the limitation, and future work are discussed in Section 5.

2. FLIGHT TRAFFIC

Enroute airspace capacity is fundamentally governed by the geometric and temporal buffers maintained between aircraft to ensure operational safety. Within Air Traffic Management (ATM) frameworks, capacity is not a static physical limit, but a dynamic threshold structurally constrained by separation standards (Pérez Maroto et al. 2022).

As air traffic volume scales, the minimum separation distances dictate the maximum density of aircraft that can safely occupy a given volume of airspace simultaneously. Consequently, any

systematic effort to optimize sector throughput or mitigate structural flight delays requires a rigorous mathematical understanding of how separation boundaries limit the mathematical capacity of the National Airspace System (NAS).

The relationship between separation distance and airspace capacity is inversely proportional; reducing the required spatial buffer inherently expands the available operational volume for routing traffic. Historically, standard enroute separation in radar-controlled environments necessitated a conservative horizontal threshold of 5 nautical miles (NM) and a vertical buffer of 2,000 feet at cruising altitudes (Pérez Maroto et al. 2022). These wide margins were critical for absorbing localized positioning errors and sensor lag associated with legacy surveillance systems. However, because aircraft must be treated as moving cylinders of prohibited airspace, these expansive static buffers artificially cap the maximum flow rate through high-demand sectors, transforming safety regulations into the primary bottleneck for enroute traffic capacity.

Advancements in digital avionics and data-driven trajectory modeling have enabled regulatory bodies to safely contract these boundaries, yielding substantial capacity gains. A premier example of this paradigm shift is the implementation of Reduced Vertical Separation Minimum (RVSM), which halved the vertical interval to 1,000 feet between flight level (FL) 290 and FL 410, effectively doubling the available cruising altitudes for properly equipped aircraft (Federal Aviation Administration 2022). Furthermore, the transition toward Automatic Dependent Surveillance-Broadcast (ADS-B) allows for highly precise, real-time state-vector tracking (Federal Aviation Administration 2022). This increased surveillance accuracy provides the empirical foundation necessary to safely shift from rigid, conservative separation constraints to dynamic, trajectory-based management, thereby maximizing contemporary airspace throughput without compromising systemic safety.

3. METHOD FOR ANALYSIS

This section describes the end-to-end pipeline used to detect, classify, and characterize pairwise proximity events (breaches) between aircraft operating in enroute airspace. The method uses a two-stage classifier for event pairs: a vertical/temporal pre-filter followed by a lateral filter to find breach pairs.

3.1 Process Overview

The full sequence of the process with 22 steps is illustrated in **Figure 1**, and the numbered list below summarizes each step in execution order, with a cross-reference to the subsection (3.1.1–3.1.8) that documents it in detail:

1. Ingest the daily ADS-B data and sort records by aircraft identifier and timestamp (Section 3.1.1).
2. Segment each aircraft's records into discrete flight legs to obtain unique flights (Section 3.1.1).
3. Filter to overhead traffic only, whose entire altitude profile stays at or above FL200 (Section 3.1.1).
4. Remove records with missing latitude, longitude, or altitude (Section 3.1.1).
5. Compute each aircraft's vertical rate directly from consecutive raw observations (Section 3.1.2).
6. Interpolate every retained leg onto a uniform 10-second time grid (Section 3.1.2).
7. At each 10-second timestamp, form every pairwise combination of aircraft (Section 3.1.3).
8. Filter pairs vertically to obtain pairs with an altitude difference of 850 ft or less (Section 3.1.3).
9. Screen the qualified pairs on lateral separation using the haversine distance (Section 3.1.3).
10. Classify each breach by severity using the nested lateral thresholds (Section 3.1.3).
11. Cross-reference every breach pair against the military aircraft database (Section 3.1.4).
12. Exclude military flights breach pairs (Section 3.1.4).
13. Classify and assign each breach to either Northbound, Southbound, or Intersecting (Section 3.1.5).
14. Classify each breach's horizontal encounter geometry and each aircraft's vertical state at the breach instant (Section 3.1.6).
15. Compute breach counts of all screened pairs by directional category and severity (Section 3.1.7).
16. Compile daily summary statistics into a master summary file (Section 3.1.7).
17. Assign each breach to a 0.5° geographic grid cell for hotspot identification (Section 3.1.7).
18. Aggregate daily breach counts by calendar month and by season (Section 3.1.7).

19. Apply the Kruskal-Wallis test and Dunn's tests with Bonferroni correction (Section 3.1.7).
20. Generate the daily separation histogram of lateral separation distributions (Section 3.1.8).
21. Generate the daily bar chart of breach counts (Section 3.1.8).
22. Export the results into a structured Excel workbook (Section 3.1.8).

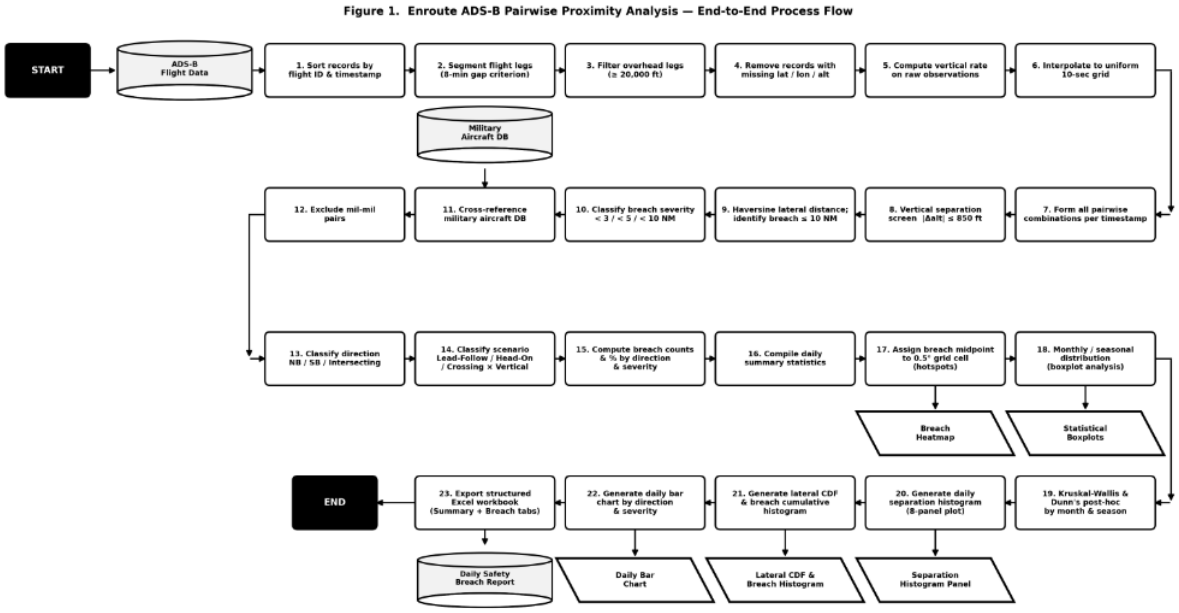


Figure 1 Process Diagram for Pairwise Flight Performance Analysis

3.1.1 Data Source and Preprocessing

The primary data source for this study was Automatic Dependent Surveillance–Broadcast (ADS-B) data, which is extensively used in aviation research to analyze aircraft trajectories, conflict detection, and operational performance (Orefice et al. 2014; Corrado, Puranik, and Mavris 2021; Thapa et al. 2023; Miyamoto et al. 2025). Flight surveillance data were collected for each day of the study period from an ADS-B data feed covering Washington DC enroute airspace at every 1-minute interval. The data had information like aircraft identifier (callsign or flight number), timestamp, latitude, longitude, altitude, ground speed, and track. Raw records were first sorted by aircraft identifier and timestamp in ascending order (Step 1).

Because a single callsign or flight number can be reused by the same aircraft across multiple unrelated trips through the surveilled volume on a given day, the data were segmented into discrete "legs" (Step 2). A new leg is declared whenever the identifier changes or whenever the gap between consecutive timestamps for the same identifier exceeds an 8-minute (480-second) threshold (Thapa and Sherry 2026). The dataset was then filtered to retain only legs whose entire altitude profile remained at or above 20,000 ft, restricting the analysis to overhead, cruise-phase traffic and excluding terminal-area arrivals, departures, and low-altitude operations (Step 3) (Thapa and Sherry 2026). Records with missing latitude, longitude, or altitude were removed (Step 4).

3.1.2 Kinematic Rate Calculation and Trajectory Interpolation

Vertical rate *VR* (feet per minute) for each aircraft was computed before interpolation, directly from consecutive raw observations within a leg, using the actual elapsed time between reports rather than the fixed 10-second grid spacing (Step 5), as shown in **Equation 1**:

$$VR = (Alt_2 - Alt_1) / (t_2 - t_1) \times 60 \quad (1)$$

Where VR is Vertical rate of aircraft, Alt is the baroaltitude for the aircraft, t_1 and t_2 are the timestamps of the two raw observations. This variable will be used for scenario analysis for vertical state of aircraft in Step 14 (Section 3.1.6).

To support pairwise comparison at common instants in time, every flight leg was resampled onto a uniform 10-second grid using linear interpolation of position, altitude, and ground speed (Step 6), as shown in **Equation 2**:

$$V = V_1 + (V_2 - V_1) \times (t - t_1) / (t_2 - t_1) \quad (2)$$

where V is the interpolated value (latitude, longitude, altitude, or ground speed) at target time t, and t_1 and t_2 are the timestamps of the two raw observations. Track angle θ was interpolated using its sine and cosine components rather than the raw angle to avoid discontinuities at the 0°/360° wraparound, as shown in **Equation 3**:

$$F = F_1 + (F_2 - F_1) \times (t - t_1) / (t_2 - t_1), \text{ where } F = \sin\theta \text{ or } \cos\theta \quad (3)$$

The interpolated track angle is then reconstructed as shown in **Equation 4**:

$$\theta = \text{atan2}(\sin\theta, \cos\theta) \quad (4)$$

3.1.3 Pairwise Combination and Separation Screening

At each 10-second timestamp, every aircraft present in the overhead traffic sample was paired with every other aircraft present at that same instant, producing the full set of pairwise combinations (Step 7). Each pair was first screened on vertical separation, computed as the absolute difference in altitude between the two aircraft (Step 8), as shown in **Equation 5**:

$$\Delta Alt = |Alt_1 - Alt_2| \quad (5)$$

Only pairs with $\Delta Alt \leq 850$ ft were retained for further analysis. This threshold is set below the 1,000-ft minimum vertical separation standard prescribed for most enroute altitudes (Federal Aviation Administration 2022).

For pairs passing the vertical screen, lateral distance was computed using the Haversine great-circle formula on the two aircraft's latitude/longitude positions, expressed in nautical miles (Sinnott 1984). A proximity breach was declared whenever lateral distance fell to 10 NM or less (Step 9). A pair of aircraft can generate multiple breaches. Within the set of detected breaches, events were further classified using three lateral thresholds: "< 3 NM", "<5 NM ", and "<10 NM" (Step 10).

3.1.4 Military Pair Exclusion

Military aircraft frequently operate under different separation procedures, in restricted or special-use airspace, or in formation, and including military-to-military pairs would bias estimates of civil enroute traffic proximity. Each aircraft pair was cross-referenced against self-developed "Flight_type Database" containing military flight information (Step 11) (Thapa and Sherry 2026). A pair was excluded from the breach population only when both aircraft in the pair were independently identified as military, either by known military aircraft type or callsign prefix (Step 12).

3.1.5 Directional Classification

Each aircraft's direction of flight was classified from its track angle at the start of its leg as Northbound (track > 270° or ≤ 90°) or Southbound (track > 90° and ≤ 270°). Breach pairs were then assigned to one of three directional categories: Northbound (both aircraft northbound), Southbound (both aircraft southbound), or Intersecting (one northbound, one southbound) (Step 13).

3.1.6 Breach Scenario Classification

For every detected breach, a descriptive scenario label was generated from the breach-instant geometry and kinematics of the two aircraft using their tracks, ground speeds, positions, and vertical rates at the moment lateral separation reached 10 NM or less.

The horizontal relationship between the two aircraft was classified using the encounter angle θ_{12}, defined as the absolute difference between the two aircraft's track angle θ, folded into the range 0–180° to handle the wraparound at due north, as shown in **Equation 6**:

$$\theta_{12} = min\ (|\theta_1 - \theta_2|,\ 360° - |\theta_1 - \theta_2|) \qquad (6)$$

Three horizontal categories were defined:

1. Lead-follow: $\theta_{12} \leq 20°$ (aircraft traveling in essentially the same direction).
2. Head-on: $\theta_{12} \geq 160°$ (aircraft traveling in essentially reciprocal directions).
3. Crossing: θ_{12} between 20° and 160° (aircraft in neither the same direction nor reciprocal).

Independently, each aircraft's vertical state at the breach instant was classified from its own instantaneous vertical rate using a ±100 ft/min threshold:

1. climbing (rate above +100 ft/min)
2. descending (rate below −100 ft/min)
3. or level (within ±100 ft/min).

A breach can combine any horizontal category with any pairing of the two aircraft's vertical states (e.g., "crossing, descending / level") (for example - "head-on, climbing"), yielding a compact but descriptive scenario label for every breach (Step 14).

3.1.7 Breach Statistical Analysis and Hotspot Identification

For each analysis day, breach counts, percentages of all screened pairs, and counts of unique aircraft pairs were computed at each of the three severity thresholds (< 3 NM, < 5 NM, < 10 NM), both overall and within each directional category (Northbound, Southbound, Intersecting) (Step 15). Daily summary statistics including overhead flight counts, total pairs, unique pairs, and per-threshold breach counts were compiled into a master summary excel file spanning the full study period (Step 16).

Geographic hotspots were identified using a 0.5° × 0.5° latitude/longitude grid, a grid-density approach consistent with established hotspot-mapping methods (Step 17). Each breach event was assigned to its containing grid cell, and breach density per cell was aggregated by direction (Northbound, Southbound, Intersecting, Overall) that highlights the geographic concentration of proximity events across the study airspace. The map also displays navigational waypoints and holding fixes within the study airspace.

Daily breach counts were aggregated by calendar month and by season to enable distributional analysis that use boxplots (Step 18). Kruskal-Wallis test was used to statistically test if seasonal and monthly variations occur for the study, based on the results from Section 4 (Step 19) (Kruskal and Wallis 1952). Post-hoc Dunn's tests with Bonferroni correction were then used to identify which seasons and months differed significantly in terms of daily breach counts (Step 19) (Dunn 1964).

3.1.8 Implementation and Outputs

The pipeline was implemented in Python using Pandas and NumPy for data processing, Openpyxl for structured Excel export, and Matplotlib for static visualization. The pipeline produces following outputs:

a. geographical location (heatmap) chart
b. boxplots by month and season.

c. Separation Histogram panel- a multi-panel histogram of lateral separation distributions for all screened pairs and for breach subsets (Step 20)
d. daily bar chart by severity threshold across all study days (Step 21)
e. Daily Safety Breach Report- an Excel workbook containing a daily summary sheet, and direction-wise, detailed sheets (Overall, Northbound, Southbound, Intersecting) (Step 22)

4. CASE STUDY

This section describes the results of an analysis of the air traffic in the Washington DC airspace defined by the boundaries latitude: 37.5, 39.38 N, longitude: 73.5, -79.11 W (**Figure 2**). This airspace includes ZDC and ZNY ARTCC. Section 4.1 describes an analysis of a single day (January 1, 2025). Section 4.2 describes an analysis of 304 days between January 1 and December 31, 2025. Missing days were due to technical difficulties in obtaining the ADS-B data.

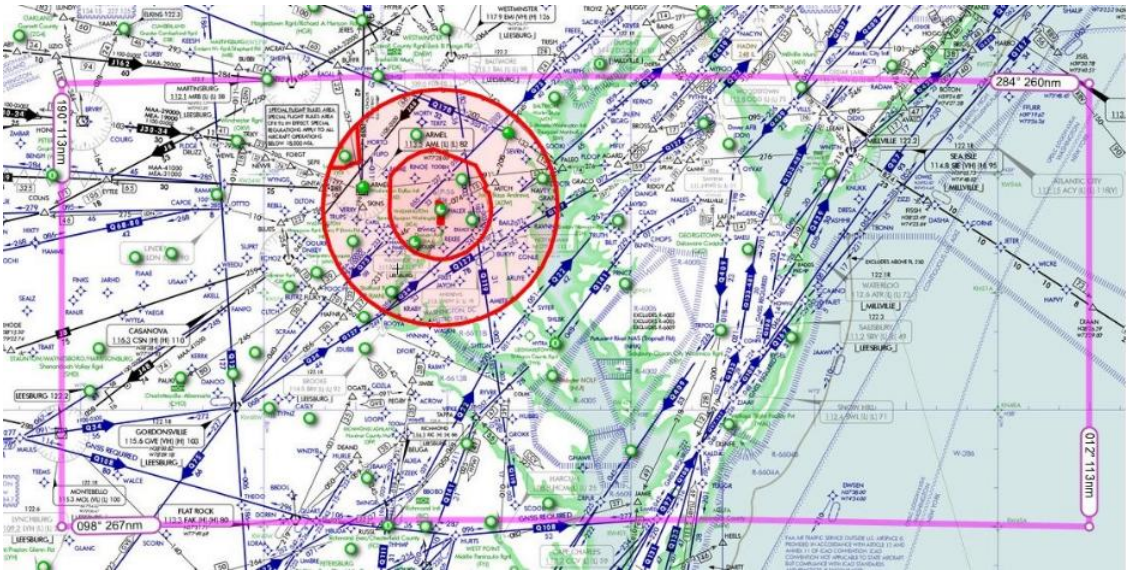


Figure 2 Bounded Airspace over the Washington DC area for the case study

The overhead flights primarily traverse the region in the north-south direction. An example of the flight tracks for January 1, 2025, is shown in **Figure 3** with directions (Northbound flights in green and Southbound flights in red).

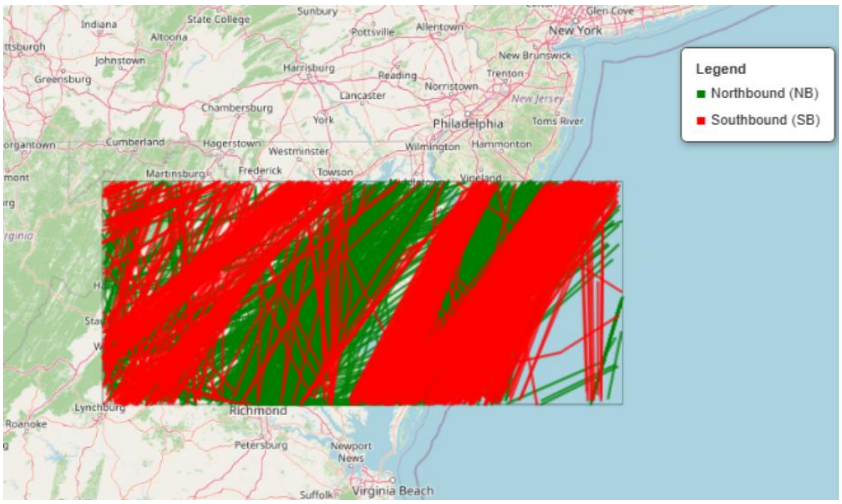


Figure 3 Washington DC bounded airspace with overhead flights for a day (January 1, 2025)

4.1 One Day Analysis

A single study day (January 1,2025) was selected to illustrate the full output of the pipeline described in Section 3. On this day, there were 2,543 overhead flights, forming 60,875 pairwise combinations that satisfied the 850 ft vertical pre-filter.

4.1.1 Breach Statistics

Of the pairs of flights that were both within +/- 850 ft, 60 distinct pairs of flights yielded 697 events with lateral separation of 10 NM or less. There were 0 events for <3 NM, 1 for <5 NM, and 697 events for <10 NM threshold (**Figure 4**).

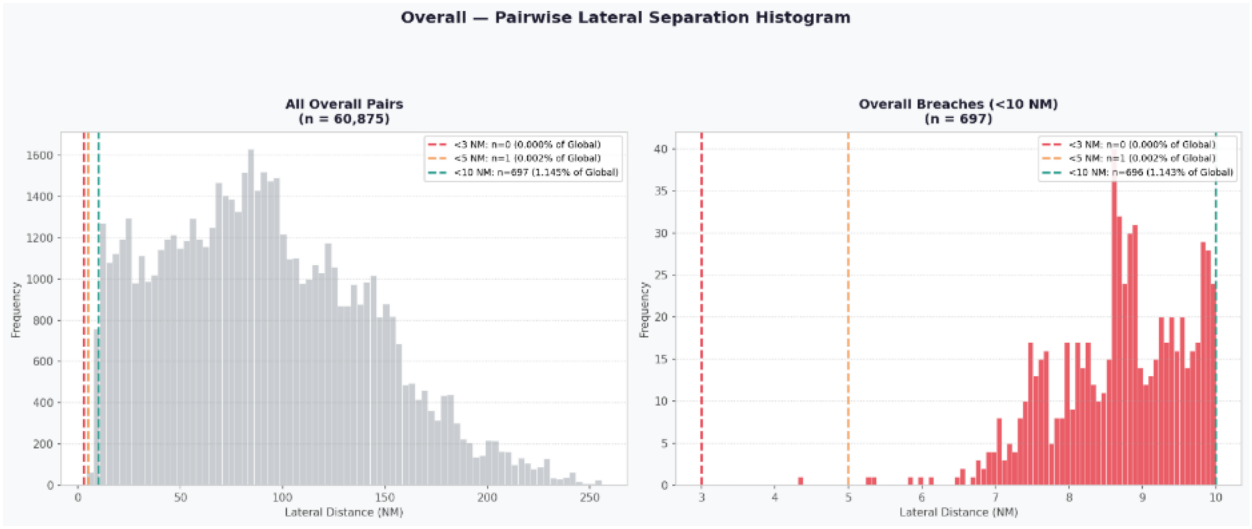


Figure 4 Overall – Pairwise Lateral Separation Histogram (January 1, 2025)

Northbound pairs accounted for the largest share of the day's breaches. 37 unique pairs of flights yielded 447 breach events. There were 0 events for <3 NM, 1 for <5 NM, and 447 events for <10 NM threshold (**Figure 5**).

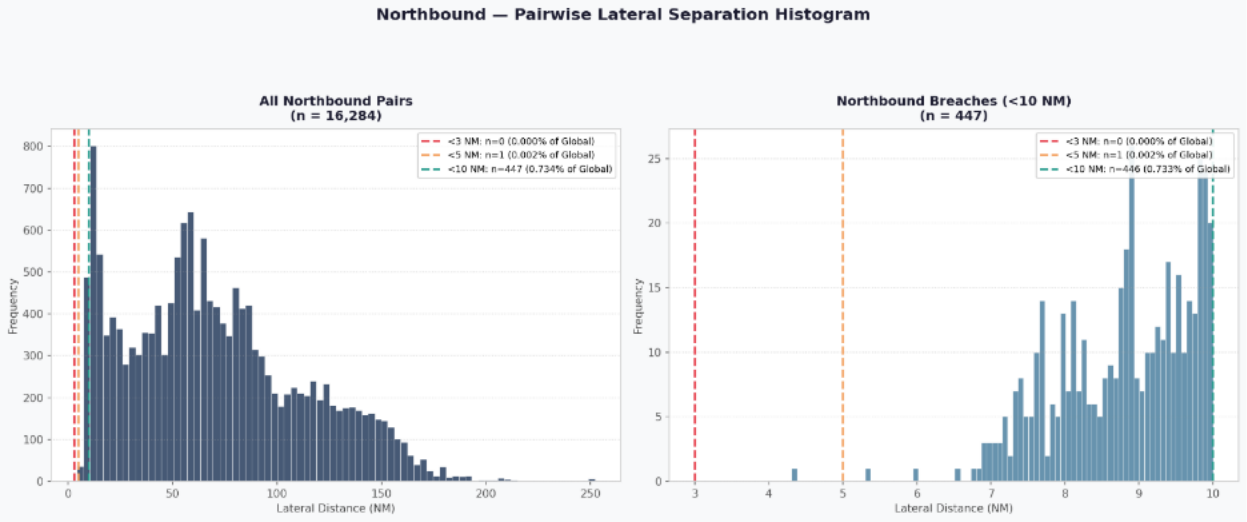


Figure 5 Northbound – Pairwise Lateral Separation Histogram (January 1, 2025)

For Southbound pairs, 15 unique pairs of flights yielded 233 breach events. There were 0 events for <3 NM, 0 for <5 NM, and 233 events for <10 NM threshold (**Figure 6**).

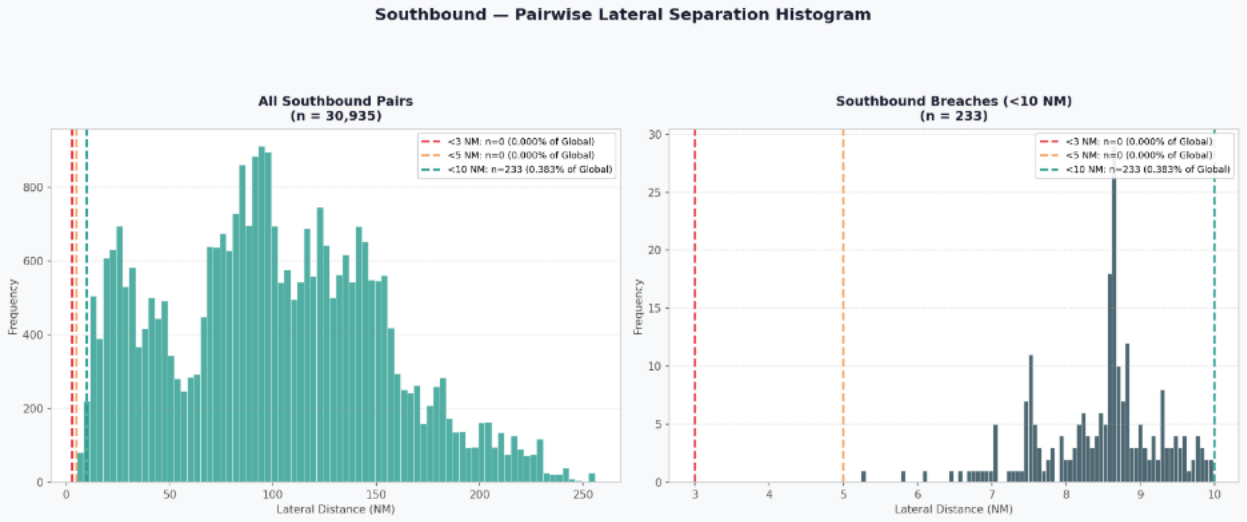


Figure 6 Southbound – Pairwise Lateral Separation Histogram (January 1, 2025)

For Intersecting pairs, 8 unique pairs of flights yielded 17 breach events. There were 0 events for <3 NM, 0 for <5 NM, and 17 events for <10 NM threshold (**Figure 7**).

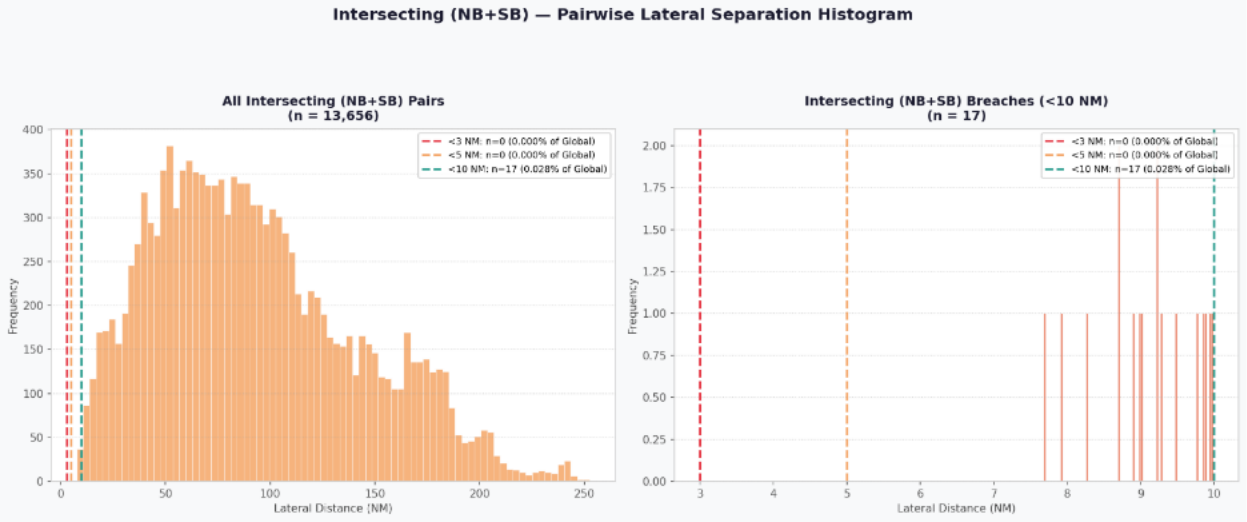


Figure 7 Intersecting – Pairwise Lateral Separation Histogram (January 1, 2025)

4.1.2 Geographic Location of Breaches

Overall (All pairs), the busiest cell containing BYSEL waypoint (see **Figure 2**) had 132 breaches (18.9% of the day's total). The second-busiest cell containing KALDA waypoint had 123 breaches (17.6% of the day's total), and the third cell containing TRPOD, had 58 breaches (8.3% of the day's total) (**Figure 8**). Together these three cells account for 44.9% of the day's 697 breaches, all of them along the coastal BYSEL–KALDA–TRPOD waypoint area.

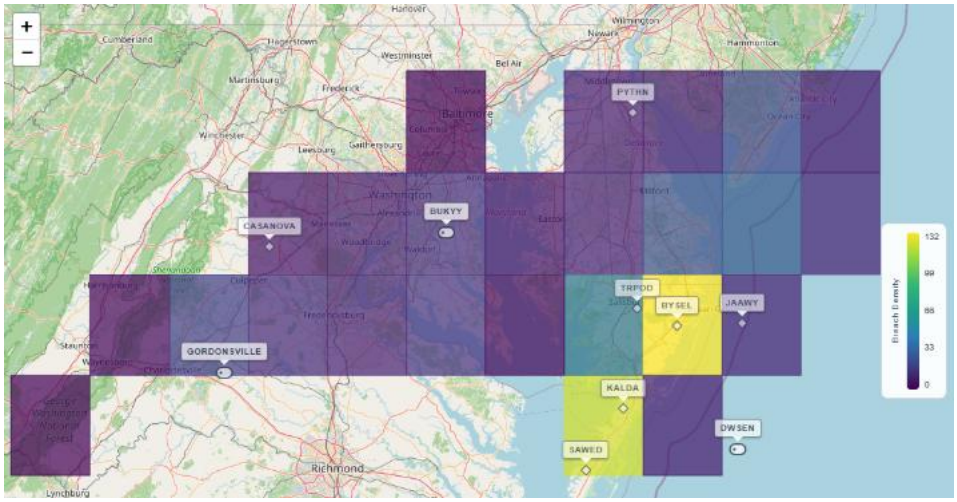


Figure 8 Overall - Geographic Location of Breaches (January 1, 2025)

Northbound pairs had 447 breaches and patterns like Overall, with the busiest cell being the same cell containing BYSEL waypoint had 129 breaches (28.9% of all Northbound breaches). The second busiest cell containing KALDA waypoint had 80 breaches (17.9%) (**Figure 9**).

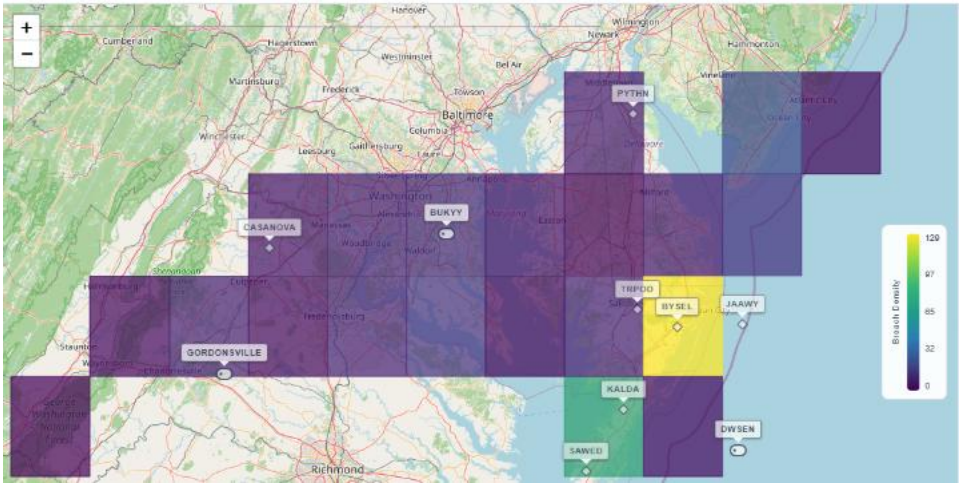


Figure 9 Northbound - Geographic Location of Breaches (January 1, 2025)

Southbound had 233 breaches in total for the day. Unlike Northbound, the busiest Southbound cell containing TRPOD had 43 breaches (18.5%), followed by the cell containing KALDA with 38 (16.3%) (**Figure 10**).

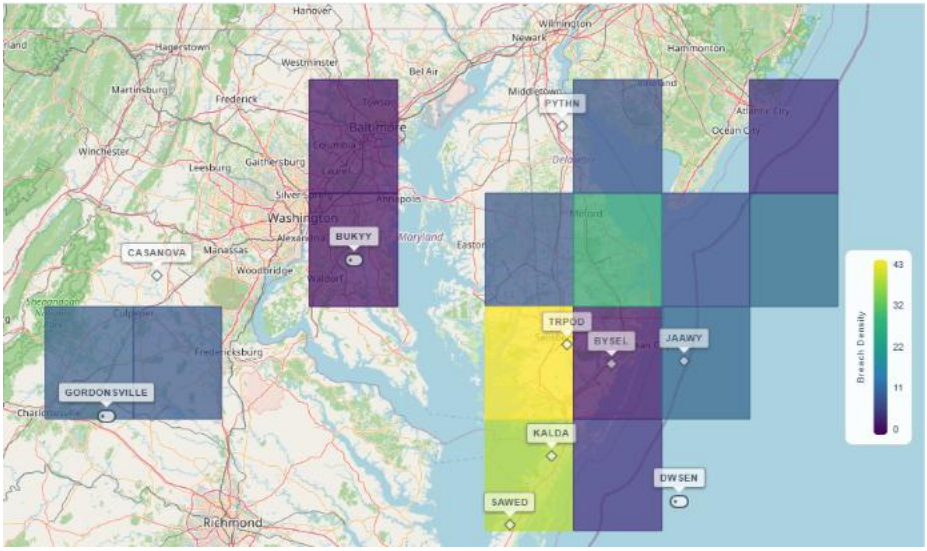


Figure 10 Southbound - Geographic Location of Breaches (January 1, 2025)

Intersecting pairs had only 17 breaches, where the busiest cell, above the JAAWY waypoint, had 10 of the 17 breaches (58.8%), with a second cell containing KALDA holding 5 (29.4%) (**Figure 11**). Both cells lie in the coastal area as the Northbound and Overall, where opposite direction airways are prevalent as seen in **Figure 2**.

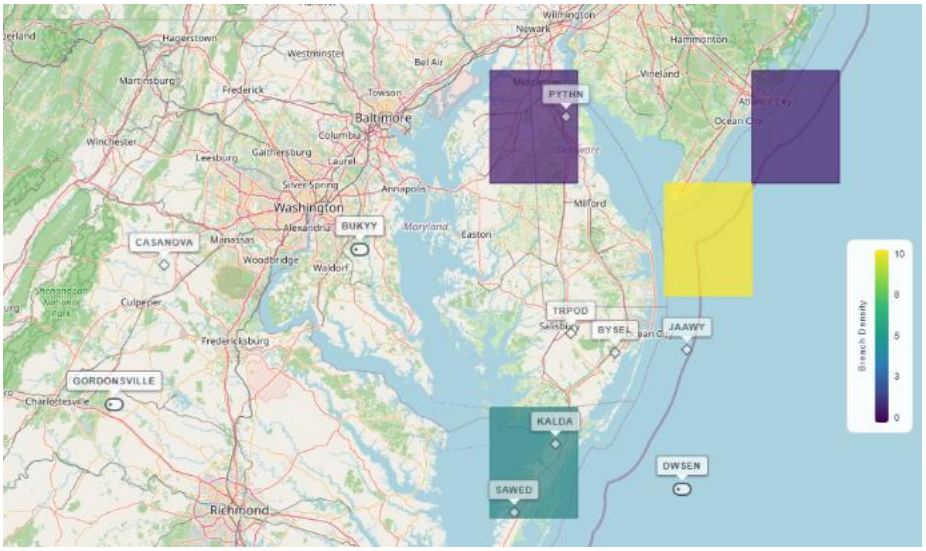


Figure 11 Intersecting - Geographic Location of Breaches (January 1, 2025)

4.1.3 Breach Geometry Scenario Statistics

The Sankey diagram shows that out of 697 breaches, 657 were lead-follow (94.3%), 23 were crossing (3.3%), and 17 were head-on (2.4%) (**Figure 12**). Out of 697, 347 were level-level (49.8%), 189 were level-descending (27.1%), 50 were descending-descending (7.2%), 108 were level-climbing (15.5%), and 3 were climbing-climbing (0.4%).

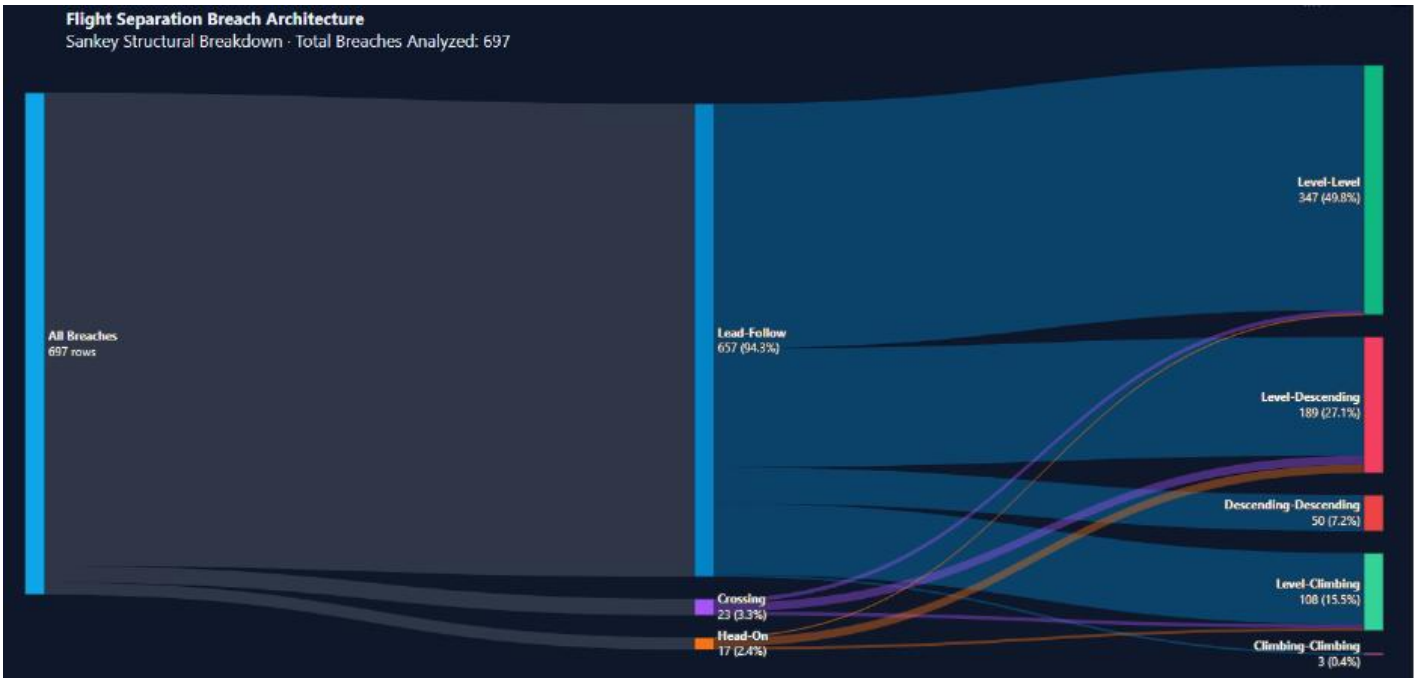


Figure 12 Sankey diagram for lateral and vertical geometries during the breaches (January 1, 2025)

4.2 Analysis of 304 Days

The full pipeline was executed for 304 days during the study period January 1 to Dec 31, 2025. Some days were missing due to technical difficulties collecting the data.

Daily Overall (<10 NM) breach counts averaged 874 per day (median 823, standard deviation 334), ranging from a minimum of 166 (September 10) to a maximum of 1,892 (March 13). By direction, Southbound pairs accounted for the largest share of overall breaches (144,999 pairs, 54.6%), followed by Northbound (111,720 pairs, 42.0%) and Intersecting (9,093 pairs, 3.4%).

4.2.1 Overall Breach Statistics

Over the full 17,600,478 pairs for 304 days, the total breach count was 265,812. There were 24 events for <3 NM (0.00014% of total pairs), 153 for <5 NM (0.00087% of total pairs), and 265,812 (1.51% of total pairs) satisfied the 10 NM threshold (**Figure 13**). All <3 NM breaches occurred in the Southbound (10) and Intersecting (14) categories, with none recorded Northbound.

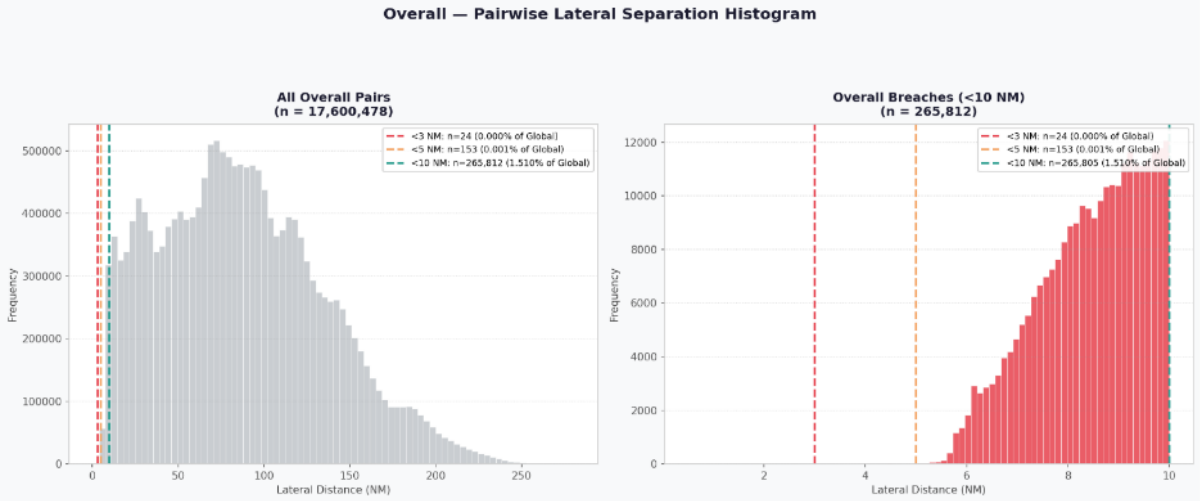


Figure 13 Overall – Pairwise Lateral Separation Histogram (2025)

For Northbound pairs, there were 0 events for <3 NM, 56 for <5 NM, and 111,720 events for <10 NM threshold (**Figure 14**).

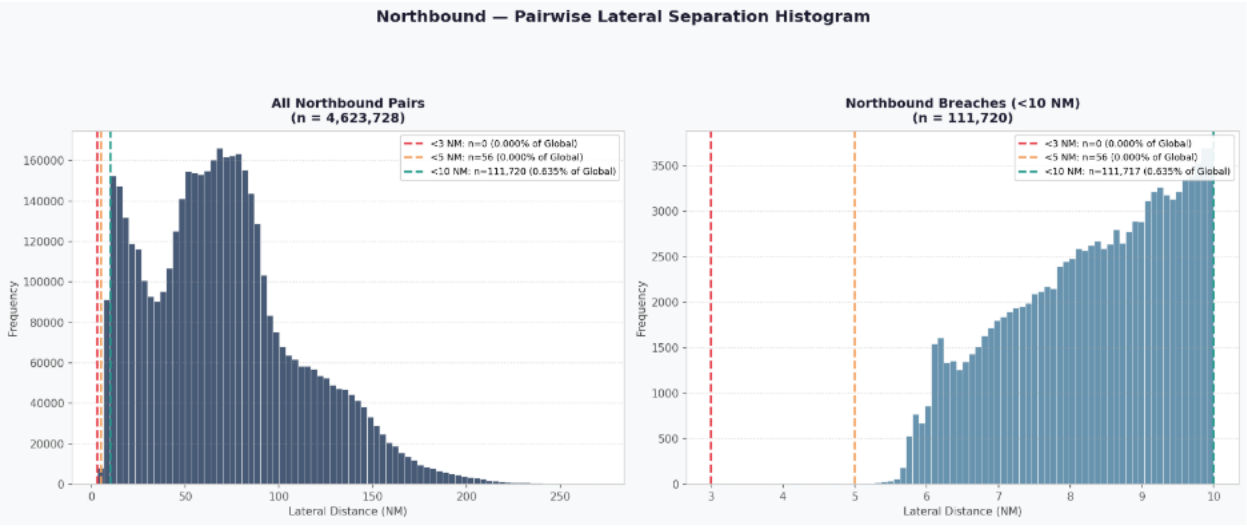


Figure 14 Northbound - Pairwise Lateral Separation Histogram (2025)

For Southbound pairs, there were 10 events for <3 NM, 43 for <5 NM, and 144,999 events for <10 NM threshold (**Figure 15**).

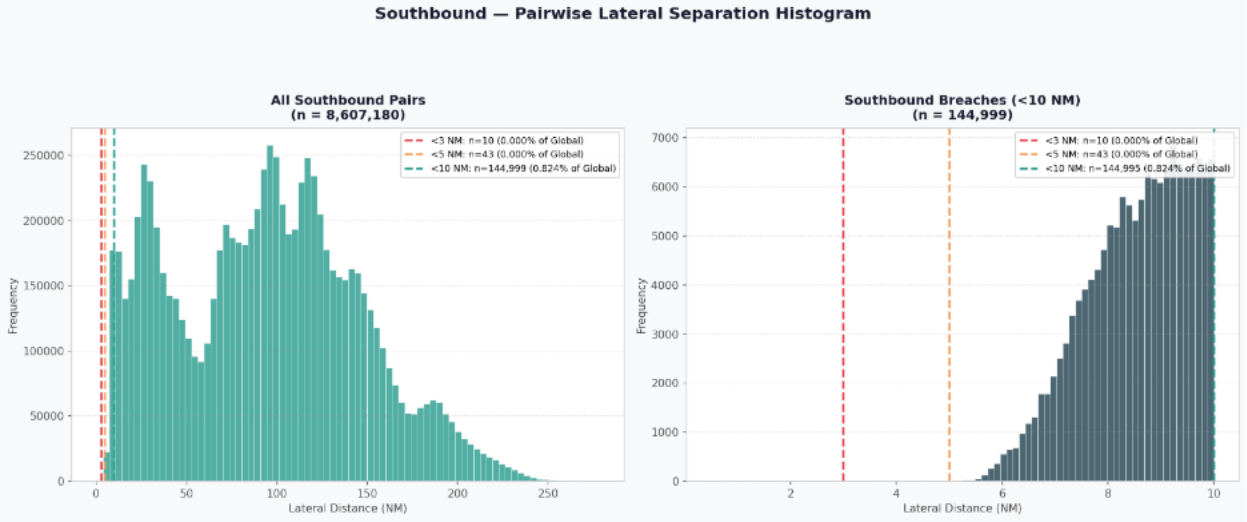


Figure 15 Southbound - Pairwise Lateral Separation Histogram (2025)

For intersecting pairs, there were 14 events for <3 NM, 54 for <5 NM, and 9,093 events for <10 NM) threshold (**Figure 16**).

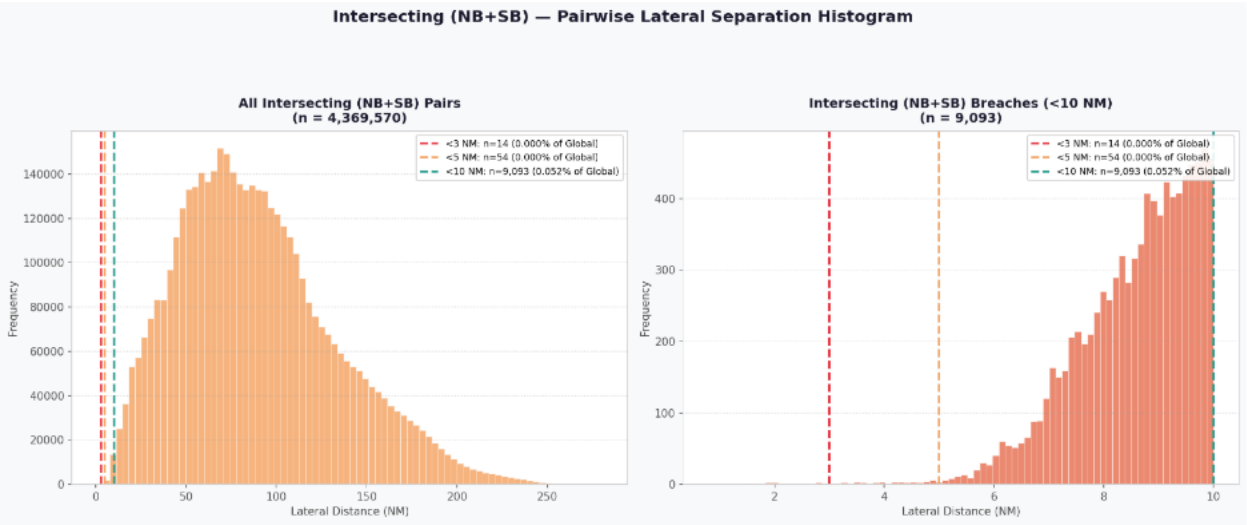


Figure 16 Intersecting – Pairwise Lateral Separation Histogram (2025)

4.2.2 Daily Breach Statistics

The < 3 NM threshold was breached on 9 of the 304 processed days (2.9%), the < 5 NM threshold on 36 of the 304 processed days (11.8%), and the < 10 NM threshold on all 304 processed days (100%) (**Table 1**).

TABLE 1 Daily statistics of safety breaches

Threshold	n (days)	Mean	Median	Min	Max
< 3 NM	9	3	2	1	8
< 5 NM	36	4	2	1	41
< 10 NM	304	874	823	166	1,892

On the days it occurred, the < 3 NM threshold averaged 3 breaches per breach-day. The median was 2, minimum was 1, and the maximum was 8 with a standard deviation of 2 (**Figure 17**). The day with the most <3 NM events was July 24, 2025.

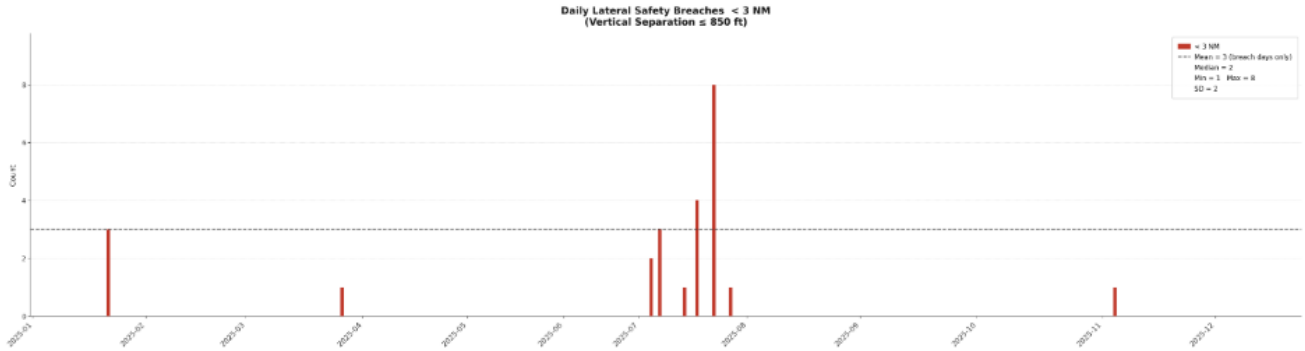


Figure 17 Bar chart of Daily Safety Breaches <3 NM (2025)

The < 5 NM threshold averaged 4 breaches per breach-day. The median was 2, minimum was 1, maximum was 41, with a standard deviation of 8 (**Figure 18**). The day with the most < 5 NM events was July 24, 2025.

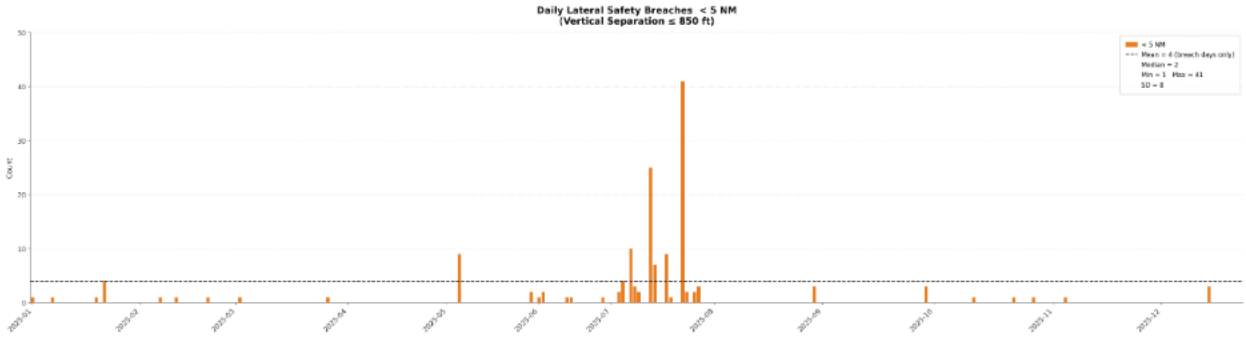


Figure 18 Bar chart of Daily Safety Breaches <5 NM (2025)

The < 10 NM threshold averaged 874 breaches per breach-day. The median was 823, minimum was 166, maximum was 1,892, with a standard deviation of 334 (**Figure 19**). The <10 NM event was present every single day for 2025.

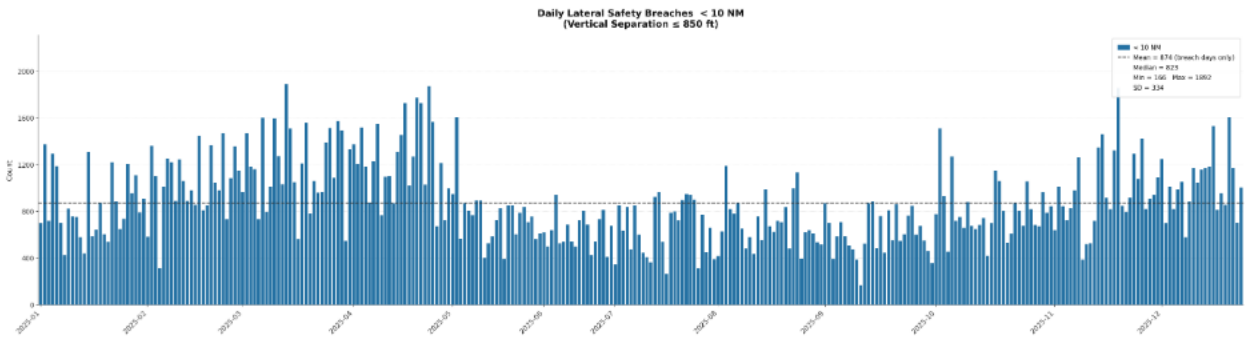


Figure 19 Bar chart of Daily Safety Breaches <10 NM (2025)

The daily breach count is right-skewed, and the variance of daily counts differs visibly across groups. The Kruskal-Wallis test was selected for statistical significance testing (Kruskal and Wallis 1952). By season, the test resulted in $H = 67.16$ ($p < 0.001$), and by calendar month, $H = 120.75$ ($p < 0.001$). In both cases, the null hypothesis is rejected, confirming that daily breach count varies by both season and month. The distribution of daily breach counts by season and by month is summarized using box-and-whisker plots (McGill et al. 1978) in **Figure 20** and **Figure 21** respectively.

Pairwise post-hoc Dunn's tests with Bonferroni correction were run on both groupings (Dunn 1964). By season, Summer differed significantly from every other season except Fall (Summer vs. Winter, $z = 6.06$, $p < 0.001$; Summer vs. Spring, $z = 7.28$, $p < 0.001$; Summer vs. Fall, $z = -2.60$, $p = 0.056$), consistent with Summer holding the lowest median (640), lowest maximum (1,188), and lowest minimum (264) daily breach count of the four seasons (**Figure 20**). Winter differed significantly from Summer and from Fall ($z = 3.72$, $p = 0.001$) but not from Spring ($z = -1.14$, $p = 1.000$); Spring, in turn, differed significantly from both Summer and Fall ($z = 4.96$, $p < 0.001$) but, as just noted, not from Winter.

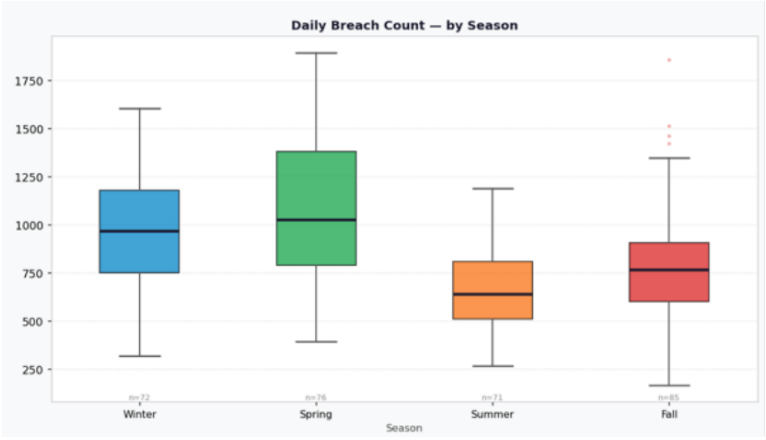


Figure 20 Boxplot of breach counts by season (2025)

By using calendar month, pairwise Dunn's tests with Bonferroni correction found that March and April each differ significantly from September (Mar–Sep, $z = 6.43$; Apr–Sep, $z = 6.68$, both $p < 0.001$) and from June, July, and August (all $p < 0.001$). September itself differs significantly from six other months, reflecting its position as the single lowest-median month of the year (**Figure 21**).

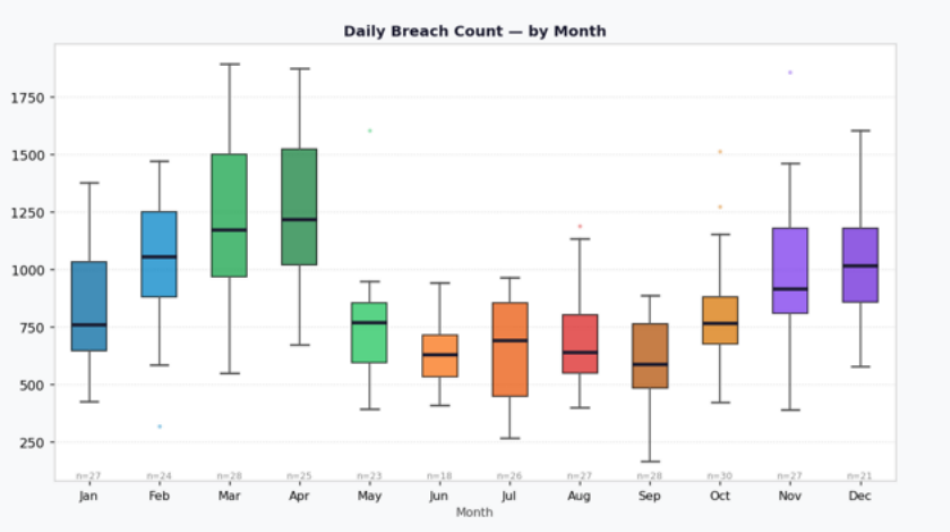


Figure 21 Boxplot of breach count by month of the year (2025)

5. CONCLUSIONS

This paper presented a statistical method for detecting, classifying, and characterizing pairwise aircraft proximity ("breach") events in enroute airspace using open-source ADS-B data. The method uses a 22-step process, with severity, directional, encounter-geometry, and vertical-state classification, and geographic hotspot mapping on a 0.5° grid.

Applied to a full year of Washington, D.C. enroute traffic (304 days, 2025), the method found that the <10 NM threshold occurred on every processed day, averaging 874 breaches per day, while the more severe <3 NM and <5 NM thresholds occurred on a much smaller subset of days (9 and 36, respectively). Daily breach counts varied significantly by both season and month (Kruskal-Wallis, $p < 0.001$ in both cases), with Summer and September consistently registering the lowest breach activity. Breaches were also not distributed uniformly in the en-route airspace, suggesting that proximity risk concentrates around specific structural or procedural features of the airspace rather than occurring uniformly across it. These results demonstrate that open-source ADS-B data, combined with a statistical pipeline, can support continuous, monitoring of separation performance in enroute airspace. The seasonal and geographic patterns identified here offer air navigation service providers a data-driven basis for safety reviews, staffing, or procedural changes for time periods and locations where proximity risk is highest, rather than applying uniform oversight across the full airspace and calendar year.

Several limitations should be noted. The analysis was limited to a single enroute airspace (Washington, D.C.) and a single calendar year, so the observed seasonal and geographic patterns may not generalize to other airspaces or years. ADS-B can be inherently subject to dropouts that were only partially addressed through the pre-filtering and interpolation steps. The ADS-B data was collected every minute, so finer data collection can avoid the necessity of interpolation.

Future work should extend this method to incorporate the Probability of Closest Point of Approach (P-CPA), which estimates conflict risk from the predicted time and distance at which two aircraft trajectories come nearest to each other, rather than relying only on discrete lateral and vertical thresholds. Extending the analysis beyond a single calendar year would also strengthen these findings. A multi-year dataset would let future work test whether the seasonal or monthly pattern found holds consistently year over year, or whether it shifts from the findings.

ACKNOWLEDGMENTS

The authors are grateful for the technical and editorial comments and suggestions from Dr John Shortle, Dr. Ran Ji, Dr. Ed Oughton, Shahab Aref, Fahimeh Ghorbani, Andrew Kirk, Erfan Ashouri, and Jon West

(GMU), Rainer Koelle, Quinten Goens. Enrico Spinelli (EuroControl), and Brian Holguin. This research was funded by the GMU Presidential Scholarship. During the preparation of this work, the author(s) used Claude AI to rephrase specific paragraphs/ and grammar. After using this tool, the author(s) reviewed and revised the content as needed and take full responsibility for the content of the publication.

AUTHOR CONTRIBUTIONS

The authors confirm contribution to the paper as follows: study conception and design: Sherry/Thapa; data collection: Thapa; analysis and interpretation of results: Thapa/Sherry; draft manuscript preparation: Thapa. All authors reviewed the results and approved the final version of the manuscript.

DECLARATION OF CONFLICTING INTERESTS

The authors declared no potential conflicts of interest with respect to the research, authorship, and/or publication of this article.

FUNDING

The authors disclosed no financial support for the research, authorship, and/or publication of this article.

REFERENCES

Corrado, Samantha J., Tejas G. Puranik, and Dimitri N. Mavris. 2021. "Characterizing Terminal Airspace Operational States and Detecting Airspace-Level Anomalies." *Engineering Proceedings* 13 (1): 9. https://doi.org/10.3390/engproc2021013009.

Dunn, Olive Jean. 1964. "Multiple Comparisons Using Rank Sums." *Technometrics* 6 (3): 241–252. https://doi.org/10.1080/00401706.1964.10490181.

Federal Aviation Administration. 2022. *Authorization of Aircraft and Operators for Flight in Reduced Vertical Separation Minimum (RVSM) Airspace*. Advisory Circular AC 91-85B. Washington, DC: U.S. Department of Transportation. https://www.faa.gov/documentLibrary/media/Advisory_Circular/AC_91-85B.pdf.

Jansen, Tim Maximilian. 2020. *Flightradar24, ADS-B and Mode S Data for Aircraft Performance Analysis*. Project report. Hamburg: Aircraft Design and Systems Group (AERO), Department of Automotive and Aeronautical Engineering, Hamburg University of Applied Sciences. https://www.fzt.haw-hamburg.de/pers/Scholz/arbeiten/TextJansen.pdf.

Kruskal, William H., and W. Allen Wallis. 1952. "Use of Ranks in One-Criterion Variance Analysis." *Journal of the American Statistical Association* 47 (260): 583–621. https://doi.org/10.1080/01621459.1952.10483441.

McGill, Robert, John W. Tukey, and Wayne A. Larsen. 1978. "Variations of Box Plots." *The American Statistician* 32 (1): 12–16. https://doi.org/10.1080/00031305.1978.10479236.

Miyamoto, Ayaka, Clement Li, Parker D. Vascik, and R. John Hansman. 2025. "ADS-B-Based Characterization of Flight Behaviors in Terminal Airspace for Safety Applications." In *AIAA AVIATION Forum and ASCEND 2025*. Reston, VA: American Institute of Aeronautics and Astronautics. https://doi.org/10.2514/6.2025-3669.

Orefice, Martina, Vittorio Di Vito, Federico Corraro, Giancarmine Fasano, and Domenico Accardo. 2014. "Aircraft Conflict Detection Based on ADS-B Surveillance Data." In *2014 IEEE International Workshop on Metrology for AeroSpace (MetroAeroSpace)*, 277–282. Piscataway, NJ: IEEE. https://doi.org/10.1109/MetroAeroSpace.2014.6865934.

Pérez Maroto, Marta, Javier García-Heras, Luis Pérez Sanz, Lidia Serrano-Mira, and Javier Alberto Pérez-Castán. 2022. "Performance Impact Assessment of Reducing Separation Minima for En-Route Operations." *Aerospace* 9 (12): 772. https://doi.org/10.3390/aerospace9120772.

Sinnott, Roger W. 1984. "Virtues of the Haversine." *Sky & Telescope* 68 (2): 158–159.

Thapa, Ashim Kumar, John Shortle, and Lance Sherry. 2023. "Air-to-Air Collision Risk Models (CRM) in the Terminal Airspace." *In 2023 Integrated Communications, Navigation and Surveillance Conference (ICNS),* 1–9. IEEE. https://doi.org/10.1109/ICNS58246.2023.10124323.

Thapa, Ashim Kumar, and Lance Sherry. 2026. "Design of a Dashboard for Enroute Traffic Operations Using Open-Source Data." In *2026 Integrated Communications, Navigation and Surveillance Conference (ICNS)*, 1–17. Piscataway, NJ: IEEE. https://doi.org/10.1109/ICNS69853.2026.11570315.